








Cite this: *RSC Adv.*, 2023, 13, 7250

# Synthesis of cationic $\beta$ -cyclodextrin functionalized silver nanoparticles and their drug-loading applications†

Ke Yang, <sup>ab</sup> Junfeng Liu, <sup>\*ab</sup> Laichun Luo, <sup>a</sup> Meilin Li, <sup>ab</sup> Tanfang Xu <sup>ab</sup> and Junfeng Zan <sup>a</sup>

Silver nanoparticles have attracted great attention owing to their distinct physicochemical properties, which inspire the development of their synthesis methodology and their potential biomedical applications. In this study, a novel cationic  $\beta$ -cyclodextrin (C- $\beta$ -CD) containing a quaternary ammonium group and amino group was applied as a reducing agent as well as a stabilizing agent to prepare C- $\beta$ -CD modified silver nanoparticles (C $\beta$ CD-AgNPs). Besides, based on the inclusion complexation between drug molecules and C- $\beta$ -CD, the application of C $\beta$ CD-AgNPs in drug loading was explored by the inclusion interaction with thymol. The formation of AgNPs was confirmed by ultraviolet-visible spectroscopy (UV-vis) and X-ray diffraction spectroscopy (XRD). Scanning electron microscopy (SEM) and transmission electron microscopy (TEM) showed the prepared C $\beta$ CD-AgNPs were well dispersed with particle sizes between 3–13 nm, and the zeta potential measurement result suggested that the C- $\beta$ -CD played a role in preventing their aggregation in solution. <sup>1</sup>H Nuclear magnetic resonance spectroscopy (<sup>1</sup>H-NMR) and Fourier transform infrared spectroscopy (FT-IR) revealed the encapsulation and reduction of AgNPs by C- $\beta$ -CD. The drug-loading action of C $\beta$ CD-AgNPs was demonstrated by UV-vis and headspace solid-phase microextraction gas chromatography mass spectrometry (HS-SPME-GC-MS), and the results of TEM images showed the size increase of nanoparticles after drug loading.

Received 25th December 2022  
Accepted 24th February 2023

DOI: 10.1039/d2ra08216k

rsc.li/rsc-advances

## Introduction

Nanomaterials, including metal/metallic oxide nanomaterials, carbon-based nanomaterials, polymeric nanomaterials, nanocomposites, *etc.* have shown great potential in biomedical areas due to their unique chemical, physical, and biological properties.<sup>1–3</sup> Among them, metal nanomaterials such as silver nanoparticles (AgNPs) have been widely investigated and employed in antibacterial, anticancer therapeutics, diagnostics, drug delivery, biosensing, and other clinical/pharmaceutical applications owing to their small particle size and large surface area.<sup>4–6</sup> Considering the potential application of AgNPs, the preparation of AgNPs has attracted significant attention in recent decades.<sup>7</sup> It has been found that the biological and chemical properties of AgNPs are related to a series of parameters including size, shape, and stability, which depend mainly on the methodology and conditions.<sup>8,9</sup> Chemical reduction of

silver salts, in the presence of chemical stabilizers and reductants, is the most common method for the synthesis of AgNPs.<sup>10,11</sup> However, the chemical method involves the use of materials that may be toxic and hazardous to the environment, with potential environmental and health concerns.<sup>12–14</sup> Recently, several biocompatible compounds, such as polymers and polysaccharides, have been used in the green synthesis of nanoparticles under environmentally friendly conditions.<sup>15–17</sup>

Cyclodextrins (CDs), a natural class of cyclic oligosaccharides produced from starch degradation, have been applied in the preparation of AgNPs.<sup>18–20</sup> CDs can serve as a reducing agent to reduce metal salts and bind to the surface of nanoparticles *via* chemisorption, thus effectively stabilizing nanoparticles.<sup>21,22</sup> Moreover, cyclodextrin derivatives have also been used in the synthesis of AgNPs due to their better properties such as great water solubility.<sup>23</sup> A. Abou-Okeil *et al.*<sup>24</sup> used aminated  $\beta$ -cyclodextrin for the preparation of AgNPs, and AgNPs with particle sizes in the range of 1–9 nm were prepared under optimal conditions. Cationic cyclodextrins have attracted interest because of their high solubility and stability.<sup>25</sup> The hydrophobic cavity and the unique ionic effects expand their applications in drug delivery and drug solubilization.<sup>26,27</sup> It has been reported that materials containing polar groups (*e.g.*, amines, hydroxyl groups, and amides) are more suitable for stabilizing nanoparticles.<sup>28</sup> Quaternary ammonium salts can stabilize Ag<sup>0</sup>

<sup>a</sup>College of Pharmacy, Hubei University of Chinese Medicine, Wuhan, 430065, P. R. China. E-mail: liujf456@hotmail.com; 1105787683@qq.com; Tel: +86-15629118698

<sup>b</sup>Key Laboratory of Traditional Chinese Medicine Resource and Compound Prescription, Ministry of Education, Hubei University of Chinese Medicine, Wuhan, 430065, P. R. China

† Electronic supplementary information (ESI) available. See DOI: <https://doi.org/10.1039/d2ra08216k>



nanoparticles through electrostatic interactions and steric effects, and the halogen ions can stabilize the Ag<sup>0</sup> nanoparticles through chelation.<sup>29</sup> As far as we know, few studies have been conducted to prepare AgNPs by using cationic cyclodextrins as reducing and stabilizing agents. In addition, their different complexation and solubilization capabilities make them an ideal host to construct inclusion complexes with guest molecules.<sup>30</sup>

Thymol (THY) is a phenol that mainly occurs in the essential oils of thyme oil, oregano oil, clove basil oil, *etc.*<sup>31</sup>. THY presents various biological activities, including antioxidant, anti-inflammatory, and antitumor activities, especially antibacterial properties, which show antibacterial and sensibility against various types of bacteria and fungi.<sup>32–34</sup> However, their poor aqueous solubility, high volatility, and sensitivity to light and heat greatly limit their application, hence it is significant to break through these limitations.<sup>35,36</sup> CD-modified AgNPs are considered a promising platform to enhance the stability and provide protection of THY from external conditions by host-guest complexation, which could broaden their potential biomedical applications.

In this study, C-β-CD functionalized AgNPs (CβCD-AgNPs) were prepared and characterized, and THY/CβCD-AgNPs nanocomposite was formed by the inclusion action of THY with CβCD-AgNPs. Herein, C-β-CD serves as a reducing agent and a stabilizing agent in the preparation of AgNPs, besides it plays a part in loading THY molecule owing to its complexation capabilities.

## Experimental

### Materials

Silver nitrate (AgNO<sub>3</sub>) and sodium hydroxide (NaOH) were purchased from Sinopharm Chemical Reagent Co. Int. β-Cyclodextrin (β-CD, 99%+) was purchased from Admas Chemical Reagent Co. Int. *p*-Toluenesulfonyl chloride (TsCl, 99%) and 2,3-epoxypropyltrimethylammonium chloride (EPTAC, 95%+) were purchased from General-Reagent Chemical Reagent Co. Int. Thymol (THY, 98%) was purchased from Aladdin Biochemical Technology Co. Int. Deionized water was obtained from ultrapure water system.

### Synthesis of C-β-CD

Two-step synthesis of DAP-β-CD: firstly, toluenesulfonyl-β-cyclodextrin (Ts-β-CD) was prepared according to the procedure reported in a previous work.<sup>37</sup> Briefly, 50.0 g of β-CD was dissolved in 500 mL of 0.4 M NaOH solution (0–5 °C), then 35.0 g of TsCl was added in batches within 5 min and stirred for another 30 min below 5 °C, after removing the unreacted TsCl by filtration, the filtrate was neutralized to pH 8 with 3 M HCl and stirred for 1 h. The resultant precipitates were filtered off, washed three times with water, and finally dried under vacuum at 40 °C. Synthesis of diaminopropane-β-cyclodextrin (DAP-β-CD) was prepared following the procedure reported in a previous<sup>38</sup> method: 4.0 g of Ts-β-CD was dissolved in 20 mL of 1,3-propanediamine and stirred at 80 °C for 4 h. Then poured

into 250 mL of EtOH. The precipitates were collected by filtration and were washed by EtOH thoroughly. The solid was dried under vacuum at 40 °C to obtain the DAP-β-CD.

C-β-CD was synthesized as follows: 0.6 g of EPTAC was dissolved in 10 mL of DMSO, subsequently, 4.5 g of DAP-β-CD was dissolved in 10 mL of DMSO solution and added to the above EPTAC solution, and then reacted at 80 °C for 4 h. Then poured into 250 mL of EtOH. The precipitates were collected by filtration and were washed by EtOH thoroughly. The solid was dried under vacuum at 40 °C to obtain the C-β-CD.

### Preparation of CβCD-AgNPs

CβCD-AgNPs were synthesized by *in situ* reduction method according to the reported method.<sup>39</sup> 5 mL of C-β-CD solution (0.01 M) was added to 32.5 mL of water, and to which 2 mL of NaOH (0.1 M) was gradually added under stirring. Upon heating the solution to 60 °C, 0.5 mL of AgNO<sub>3</sub> solution (0.1 M) was added dropwise, and the solution was further reacted for 1 h at 60 °C to obtain CβCD-AgNPs. The resulting AgNPs were collected by centrifugation and washed three times with deionized water.

### Preparation of THY/CβCD-AgNPs composite

THY/CβCD-AgNPs complex solution was obtained by slowly adding 5 mL of THY solution (0.01 M) to the CβCD-AgNPs solution and stirring for 24 h at 25 °C. The resulting nanoparticles were collected by centrifugation and washed three times with deionized water.

### Characterization

<sup>1</sup>H-NMR spectrum was conducted on a Bruker Avance 600 M NMR instrument by using D<sub>2</sub>O as solvent. FT-IR spectrum was measured on a Nicolet 6700 Fourier external spectrometer. The samples were mixed with KBr and pressed into pellets. A total of 32 scans were acquired, ranging from 4000 to 400 cm<sup>−1</sup> at a resolution of 4 cm<sup>−1</sup>. The UV-vis absorption spectrum was recorded by N60 Implen UV-visible spectrophotometer, and samples for UV-vis spectra analysis were prepared by mixing 1 mL of the solution in 10 mL of water. XRD pattern was measured on an XD6 X-ray diffractometer at 40 kV and 30 mA with a scanning speed of 5° per min and a scanning range of 20°–90° by using Cu Kα radiation (λ = 0.1546 nm). TEM was carried out on a JEM-1400 transmission electron microscope operated at an acceleration voltage of 80 kV, the TEM samples were prepared by placing a few drops of as-prepared sol on the surface of the copper mesh covered with a carbon support film, and dried at room temperature. The particle size distribution was obtained from the TEM image with the ImageJ software. Nanoparticle morphology was determined using a JSM-6510LV scanning electron microscope. The samples were attached to the conductive adhesive surface and observed at an accelerating voltage of 15 kV. Zeta potential measurement was performed using a Nano S90 Malvern Zetasizer at 25 °C, and the average of the three test results was taken as the reported value. GC-MS analysis was tested in Trace GC Ultra-ISQ MS with SPME equipment.



## Results and discussion

### Synthetic route and structure characterization of C- $\beta$ -CD

C- $\beta$ -CD was synthesized as shown in Scheme 1. The reaction of  $\beta$ -CD with TsCl under alkaline conditions afforded Ts- $\beta$ -CD, which underwent nucleophilic substitution with 1,3-propanediamine to obtain DAP- $\beta$ -CD. Finally, an epoxide ring-opening reaction of EPTAC with DAP- $\beta$ -CD afforded the desired C- $\beta$ -CD.

The FT-IR spectra of the cyclodextrin derivatives were shown in Fig. 1A. The characteristic peaks of Ts- $\beta$ -CD at 1364.79  $\text{cm}^{-1}$ , 1178.90  $\text{cm}^{-1}$ , and 650–900  $\text{cm}^{-1}$  disappeared from the DAP- $\beta$ -CD while showing N–H deformation vibration at 1570  $\text{cm}^{-1}$ , and C–N stretching vibration peak at 1080  $\text{cm}^{-1}$ . These results indicated that Ts- $\beta$ -CD has been successfully converted to DAP- $\beta$ -CD by nucleophilic substitution reaction. In addition, the cyclodextrin backbone of C- $\beta$ -CD was retained with O–H stretching vibration and N–H stretching vibration peaks at 3379  $\text{cm}^{-1}$  and C–H stretching vibration at 2927  $\text{cm}^{-1}$ . Besides, the N–H deformation vibration peak at 1570  $\text{cm}^{-1}$  was weakened, while the bending vibration of  $-\text{CH}_3$  in the quaternary ammonium salt substituent group appeared at 1413  $\text{cm}^{-1}$ , thus confirming the EPTAC was incorporated onto  $-\text{NH}_2$  of DAP- $\beta$ -CD and C- $\beta$ -CD was successfully synthesized.

To further confirm the successful synthesis of the cationic cyclodextrin, the specific characterization of DAP- $\beta$ -CD and C- $\beta$ -CD was examined by  $^1\text{H}$  NMR analysis. As shown in Fig. 1B, DAP- $\beta$ -CD showed signals at 5.07–3.64 ppm corresponding to the cyclodextrin glucopyranose unit (H1–6), and the signals at 2.87–2.59 ppm, 1.74–1.60 ppm, and 1.60–1.60 were attributed to the methylene of 1,3-propanediamine. These observations provided strong evidence that the amino group of 1,3-propanediamine was successfully substituted on cyclodextrin backbones. C- $\beta$ -CD showed the proton signal at 3.24 ppm represented the methyl of the quaternary ammonium branched chain, the signals at 3.47–3.35 ppm referred to the H11–12 of the cationic group, and signals appeared at 2.47–3.35 ppm that resulted from the methylene of H7 and H9–10 that attached to the N atom, which indicated the formation of cationic cyclodextrin.  $^{13}\text{C}$  NMR and MS analysis data can be found in the ESI†.

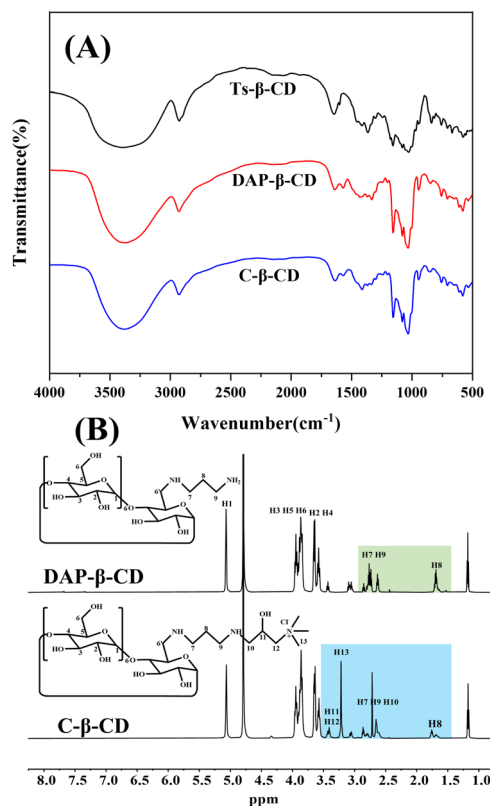
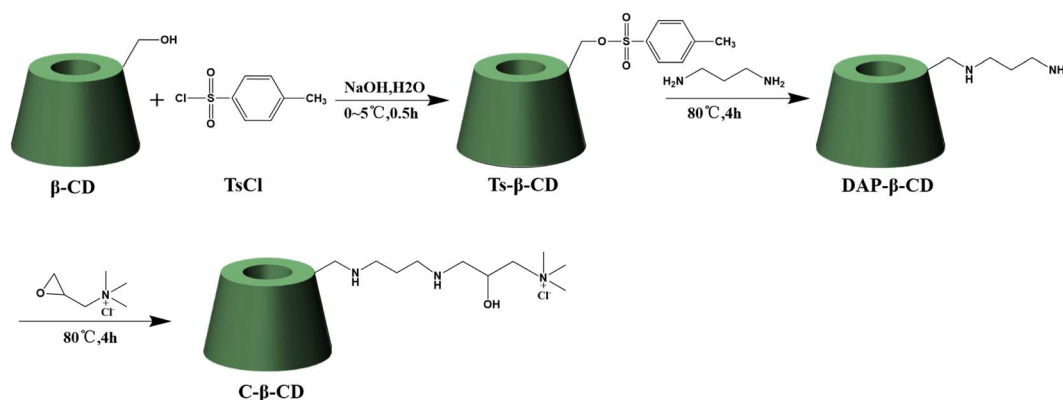


Fig. 1 FT-IR spectrum of Ts- $\beta$ -CD, DAP- $\beta$ -CD, and C- $\beta$ -CD (A),  $^1\text{H}$ -NMR spectrum of DAP- $\beta$ -CD and C- $\beta$ -CD (B).

### Synthesis and characterization of C $\beta$ CD-AgNPs

CDs are natural macrocycles composed of D-glucopyranose units that have been exploited for the synthesis of AgNPs. Under alkaline conditions, CDs can serve as a reducer and stabilizer, catalyze the reduction of  $\text{Ag}^+$  to metallic  $\text{Ag}^0$ , and prevent agglomeration of AgNPs.<sup>40</sup> Since cationic cyclodextrins have different complexation and solubilization abilities compared with other CD derivatives. The amino groups and quaternary ammonium groups play a role in reducing and stabilizing AgNPs. C- $\beta$ -CD is an ideal reducing and stabilizing agent in the



Scheme 1 The synthetic route of C- $\beta$ -CD.

synthesis of AgNPs. The synthesis scheme of the C $\beta$ CD-AgNPs is illustrated in Scheme 2.

The reaction mixture showed color changes from initially colorless to yellowish gray and eventually yellowish brown as the reaction time increases, indicating the formation of C $\beta$ CD-AgNPs. UV-vis spectroscopy is widely applied for the characterization of C $\beta$ CD-AgNPs. Besides, it has been proposed that the absorption peaks can characterize the surface plasmon resonance effect of the nanoparticles, and the morphology of AgNPs was correlated with the position of its maximum absorption peak. The absorption peak appeared at 410 nm, indicating that the prepared nanoparticles were roughly spherical. The UV-vis absorption spectrum of the synthesized C $\beta$ CD-AgNPs is shown in Fig. 2a, the synthesized C $\beta$ CD-AgNPs exhibited a typical plasma band at 402 nm, which confirmed the successful preparation of spherical AgNPs.

TEM and SEM were carried out to observe the morphology, size, and dispersity of the fabricated C $\beta$ CD-AgNPs. The SEM image is shown in Fig. 2b, in which the nearly spherical AgNPs were distributed in irregular plates. As shown in Fig. 2c, the TEM image showed the C $\beta$ CD-AgNPs were mainly subspherical in shape. The histogram showed a narrow distribution of particle size, as the particle size concentrated in the range of 3 to 13 nm, with an average particle size of  $7.60 \pm 2.14$  nm. It is concluded that the lone pair of electrons on the N of the amine group provided an electron source for the reduction of Ag $^+$  and played a role in the reduction and complexation of Ag $^+$  in the synthesis of C $\beta$ CD-AgNPs. Besides, obvious agglomeration has not appeared in the C $\beta$ CD-AgNPs, it may be a result of the positively charged quaternary ammonium group which prevented the aggregation of C $\beta$ CD-AgNPs through electrostatic repulsion.

The crystal structure of C $\beta$ CD-AgNPs was characterized by the XRD technique. The XRD spectrum of C $\beta$ CD-AgNPs showed sharp peaks indicating good crystallinity of the synthesized C $\beta$ CD-AgNPs. The diffraction peaks at  $38.18^\circ$ ,  $44.40^\circ$ ,  $64.80^\circ$ ,  $77.96^\circ$ , and  $81.52^\circ$  (Fig. 2d), corresponding to face-centered cubic crystalline singlets (111), (200), (220), (311), and (222) crystallographic planes of silver, further confirming the presence of C $\beta$ CD-AgNPs. The quaternary ammonium cation group modified in the C- $\beta$ -CD structure may contain a certain concentration of Cl $^-$ , however, no diffraction peaks of AgCl were found in the synthesized C $\beta$ CD-AgNPs. It was speculated that the hydroxyl group could compete with Cl $^-$  for Ag $^+$  under the

protection of the cyclodextrin hydroxyl group and alkaline conditions, allowing the C $\beta$ CD-AgNPs to be stable.<sup>41</sup>

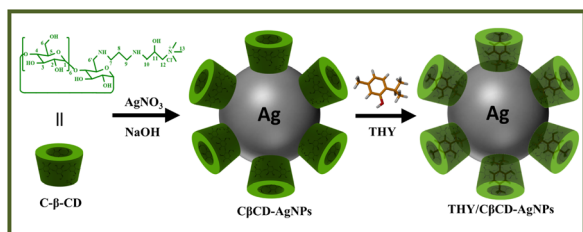
To investigate the interaction between C- $\beta$ -CD and AgNPs, C- $\beta$ -CD and C $\beta$ CD-AgNPs were determined by FT-IR (Fig. 2e). The C- $\beta$ -CD spectrum showed bands at  $3377\text{ cm}^{-1}$  (stretching vibration of N-H and O-H), and  $2929\text{ cm}^{-1}$  (C-H stretching vibration),  $1032\text{ cm}^{-1}$  (C-O-C-glycoside bridge asymmetric expansion vibration peaks), and the N-H deformation vibration peak at  $1570\text{ cm}^{-1}$ . The spectrum of C $\beta$ CD-AgNPs showed a red shift of the O-H stretching vibration band at  $3377\text{ cm}^{-1}$  to  $3422\text{ cm}^{-1}$ , indicating the deprotonation of the -OH of C- $\beta$ -CD in alkaline solution, which facilitates the synthesis and stabilization of AgNPs.<sup>42</sup> The N-H deformation vibrational peak of C- $\beta$ -CD at  $1570\text{ cm}^{-1}$  was slightly weakened, suggesting that the amine group may interact with Ag $^+$  and participate in the reduction and stabilization of AgNPs. Moreover, the peak that appeared at  $1626$  and  $1383\text{ cm}^{-1}$  may be attributed to COO $^-$  stretching vibration, which could be a result of the Ag-COO $^-$  interaction. The hydroxyl groups of C- $\beta$ -CD act as a reducing agent to reduce Ag $^+$  to AgNPs, and they were self-oxidized to carboxylic acid.<sup>43</sup> The primary OH-6 groups are more readily exposed to the chemical environment compared to the secondary hydroxyl groups, for the reason that one glucose OH-3 group interacts with the adjacent glucose OH-2 group to form intramolecular hydrogen bonds.<sup>44,45</sup> Moreover, it has been reported that, at pH 10–12, the secondary hydroxyl of  $\beta$ -CD is not oxidized, and no dioxirane formation is formed,<sup>42</sup> which indicates that the chemisorption occurs *via* these primary hydroxyl groups.

The interaction between AgNPs and C- $\beta$ -CD was investigated using  $^1\text{H}$ -NMR spectroscopy. The overlapping images of the  $^1\text{H}$  NMR spectra of both were shown in Fig. 2f, it was indicated that the proton signals of C- $\beta$ -CD appeared in C $\beta$ CD-AgNPs following a significant variation of chemical shift, which attributed to the shielding effect of the interaction of AgNPs with C- $\beta$ -CD.

Zeta potential measurement is essential to test the stability of C $\beta$ CD-AgNPs in aqueous suspensions, and a zeta potential less than  $-25\text{ mV}$  or greater than  $+25\text{ mV}$  usually has high stability.<sup>46</sup> The synthesized C $\beta$ CD-AgNPs showed a surface charge of  $-34.43 \pm 0.84\text{ mV}$ , indicating that the C $\beta$ CD-AgNPs solutions were relatively stable.

### Synthesis and characterization of THY/C $\beta$ CD-AgNPs

CDs are extensively used in nanocomposites and metallic nanoparticles as they may influence the characteristics of nanoparticles, such as drug loading, solubility, stability, and bioavailability.<sup>47</sup> The C- $\beta$ -CD has a characteristic structure and unique ability, which allows it to form inclusion complexation with drug molecules *via* the non-covalent interaction. Hence, C $\beta$ CD-AgNPs were employed in loading thymol (THY), a natural phenolic compound with numerous biological activities, which could enhance the solubility and bioavailability of THY. The synthesis scheme of the THY/C $\beta$ CD-AgNPs is shown in Scheme 2.



Scheme 2 Schematic representation for the synthesis of C $\beta$ CD-AgNPs and THY/C $\beta$ CD-AgNPs.



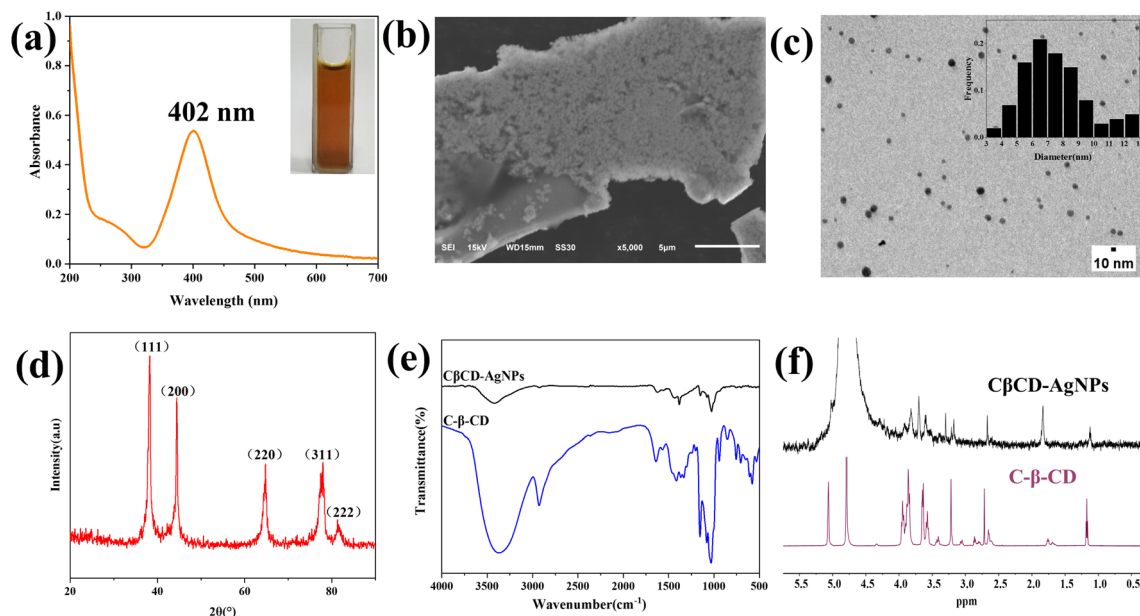


Fig. 2 UV-vis spectrum of C $\beta$ CD-AgNPs (a), SEM image of C $\beta$ CD-AgNPs (b), TEM image of C $\beta$ CD-AgNPs (c), XRD pattern of C $\beta$ CD-AgNPs (d), FT-IR spectrum of C $\beta$ CD-AgNPs (e),  $^1\text{H}$ -NMR spectrum of C $\beta$ CD-AgNPs and C- $\beta$ -CD (f).

Fig. 3A shows the distribution of THY/C $\beta$ CD-AgNPs in a colloidal solution. 100 spherical nanoparticles were randomly selected for the size statistics analysis, and the size distribution histogram showed that the particle size distribution in the whole solution ranged from 6 nm to 20 nm, with an average particle size of  $12.82 \pm 2.60$  nm. The surface charge measured for the THY/C $\beta$ CD-AgNPs is  $-30.20 \pm 0.26$  mV, which is relatively decreased compared to the C $\beta$ CD-AgNPs, indicating the aggregation of nanoparticles that may be caused by the inclusion of THY. The THY/C $\beta$ CD-AgNPs samples were extracted by ethanol ultrasonication, and the UV-vis spectra of THY and the supernatant of THY/C $\beta$ CD-AgNPs after centrifugation were shown in Fig. 3B. The UV absorption characteristics of THY were noticeable in the alcohol solution obtained after extraction, which proved the effective encapsulation of THY by C $\beta$ CD-AgNPs. HS-SPME-GC-MS analysis was applied to further verify the inclusion of THY in C $\beta$ CD-AgNPs, and the results are shown

in Fig. 3C, THY was detected and identified in THY/C $\beta$ CD-AgNPs samples at a retention time of 15.91 min (Fig. 3D).

## Conclusions

Spherical and stable AgNPs were successfully synthesized using C- $\beta$ -CD as a reducing as well as a stabilizing agent. The abundant hydroxyl groups and amino groups of C- $\beta$ -CD could effectively reduce and stabilize the nanoparticles under alkaline conditions as indicated by UV-vis, XRD, FT-IR, and zeta potential measurements. In addition, the obtained C $\beta$ CD-AgNPs were employed in loading THY molecules by virtue of the inclusion ability of C- $\beta$ -CD. THY/C $\beta$ CD-AgNPs were prepared and characterized through UV-vis and HS-SPME-GC-MS. Hence, C- $\beta$ -CD plays a dual role in the synthesis of AgNPs and drug loading. This work not only extended the application of cationic cyclodextrin derivatives in the synthesis of metal nanoparticles, but

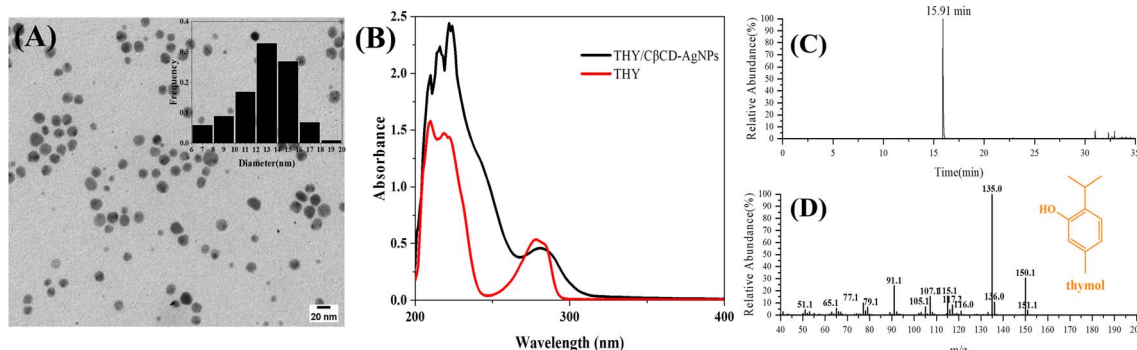


Fig. 3 TEM images of THY/C $\beta$ CD-AgNPs (A), UV-vis spectra of THY/C $\beta$ CD-AgNPs and THY (B), HS-SPME-GC-MS base peak chromatogram of THY/C $\beta$ CD-AgNPs (C), mass spectrum of THY (D).



also investigated the drug-loading effects of cationic cyclodextrin functionalized AgNPs, which have potential biomedical applications in antibacterial and drug delivery. Furthermore, the positive charge possessed by the C- $\beta$ -CD can be used for self-assembly with negatively charged polymeric materials, thus leading to the development of new materials with better performance and multiple functions.

## Author contributions

KY performed the synthesis of C- $\beta$ -CD and C $\beta$ CD-AgNPs, preparation of THY/C $\beta$ CD-AgNPs composite, FT-IR, XRD, TEM, SEM, Zeta potential measurement experimental work,  $^1\text{H}$ -NMR spectrum and all experimental data analysis under the supervision of JL. LL performed the optimization of the synthesis method. ML and TX performed the UV-vis spectra, HS-SPME-GC/MS, and TEM data analysis under the supervision of JL and JZ. All authors contributed to the interpretation of data. The manuscript was written by KY and JL through contributions from KY, JL, LL, ML, TX and JZ.

## Conflicts of interest

The authors declare no conflicts to declare.

## Acknowledgements

This work was financially supported by Special Research Foundation for Doctoral Program of Higher Education, Ministry of Education (20124230120004) and Key Project Cultivation Program of Hubei University of Chinese Medicine (2019ZXZ002).

## Notes and references

- 1 L. Hong, S. H. Luo, C. H. Yu, Y. Xie, M. Y. Xia, G. Y. Chen and Q. Peng, *Pharm. Nanotechnol.*, 2019, **7**, 129–146.
- 2 S. Islam, D. Thangadurai, C. O. Adetunji, O. S. Michael, W. Nwankwo, O. Kadiri, O. A. Anani, S. Makinde and J. B. Adetunji, in *Handbook of Nanomaterials and Nanocomposites for Energy and Environmental Applications*, eds. O. V. Kharissova, L. M. Torres-Martínez and B. I. Kharisov, Springer International Publishing, Cham, 2021, pp. 117–134.
- 3 L. Liu, C. Ge, Y. Zhang, W. Ma, X. Su, L. Chen, S. Li, L. Wang, X. Mu and Y. Xu, *Biomater. Sci.*, 2020, **8**, 4852–4860.
- 4 A. Naganthran, G. Verasoundarapandian, F. E. Khalid, M. J. Masarudin, A. Zulkharnain, N. M. Nawawi, M. Karim, C. A. Che Abdullah and S. A. Ahmad, *Materials*, 2022, **15**, 427.
- 5 S. Qamer, M. H. Romli, F. Che-Hamzah, N. Misni, N. M. S. Joseph, N. A. AL-Haj and S. Amin-Nordin, *Molecules*, 2021, **26**, 5057.
- 6 S. H. Lee and B.-H. Jun, *Int. J. Mol. Sci.*, 2019, **20**, 865.
- 7 N. Tehri, A. Vashishth, A. Gahlaut and V. Hooda, *Inorg. Nano-Met. Chem.*, 2020, 1–19.
- 8 P. Li, S. Li, Y. Wang, Y. Zhang and G.-Z. Han, *Colloids Surf., A*, 2017, **520**, 26–31.
- 9 V. I. Bhoi, S. Kumar and C. N. Murthy, *New J. Chem.*, 2016, **40**, 1396–1402.
- 10 J. Suárez-Cerda, G. A. Nuñez, H. Espinoza-Gómez and L. Z. Flores-López, *Mater. Sci. Eng.*, 2014, **43**, 21–26.
- 11 L. Xu, Y.-Y. Wang, J. Huang, C.-Y. Chen, Z.-X. Wang and H. Xie, *Theranostics*, 2020, **10**, 8996–9031.
- 12 S. Dawadi, S. Katuwal, A. Gupta, U. Lamichhane, R. Thapa, S. Jaisi, G. Lamichhane, D. P. Bhattarai and N. Parajuli, *J. Nanomater.*, 2021, **2021**, 1–23.
- 13 A. Mekkiawy, M. El-Mokhtar, N. Nafady, N. Yousef, M. Hamad, S. El-Shanawany, E. Ibrahim and M. Elsabahy, *Int. J. Nanomed.*, 2017, **12**, 759–777.
- 14 V. Demchenko, S. Riabov, S. Sinelnikov, O. Radchenko, S. Kobylinskyi and N. Rybalchenko, *Carbohydr. Polym.*, 2020, **242**, 116431.
- 15 Y. Jing, J. Li, Y. Zhang, R. Zhang, Y. Zheng, B. Hu, L. Wu and D. Zhang, *Int. J. Biol. Macromol.*, 2021, **183**, 1317–1326.
- 16 I. Medina-Ramírez, S. Bashir, Z. Luo and J. L. Liu, *Colloids Surf., B*, 2009, **73**, 185–191.
- 17 W. Jian, M. Hou, H. Wu, Y. Ma, L. Lin, B. Jia, X. Shen, H. Xiong and W. Wang, *Carbohydr. Polym.*, 2020, **245**, 116576.
- 18 A. Pandey, *Environ. Chem. Lett.*, 2021, **19**, 4297–4310.
- 19 R. Gannimani, M. Ramesh, S. Mtambo, K. Pillay, M. E. Soliman and P. Govender, *J. Inorg. Biochem.*, 2016, **157**, 15–24.
- 20 G. Cutrone, J. M. Casas-Solvas and A. Vargas-Berenguel, *Int. J. Pharm.*, 2017, **531**, 621–639.
- 21 S. Jaiswal, B. Duffy, A. K. Jaiswal, N. Stobie and P. McHale, *Int. J. Antimicrob. Agents*, 2010, **36**, 280–283.
- 22 S. Sadjadi, F. Ghoreyshi Kahangi, M. Dorraj and M. M. Heravi, *Molecules*, 2020, **25**, 241.
- 23 G. Angelini and C. Gasbarri, *Colloids Surf., A*, 2022, **633**, 127924.
- 24 A. Abou-Okeil, A. Amr and F. A. Abdel-Mohdy, *Carbohydr. Polym.*, 2012, **89**, 1–6.
- 25 J. R. Lakkakula, T. Matshaya and R. W. M. Krause, *Mater. Sci. Eng.*, 2017, **70**, 169–177.
- 26 J. Xin, Z. Guo, X. Chen, W. Jiang, J. Li and M. Li, *Int. J. Pharm.*, 2010, **386**, 221–228.
- 27 L. Huang, J. Xin, Y. Guo and J. Li, *J. Appl. Polym. Sci.*, 2010, **115**, 1371–1379.
- 28 S. S. Mahapatra and N. Karak, *Mater. Chem. Phys.*, 2008, **112**, 1114–1119.
- 29 J. Xiao, Z. Wu, K. Li, Z. Zhao and C. Liu, *RSC Adv.*, 2022, **12**, 1051–1061.
- 30 F. Gómez-Galván, L. Pérez-Álvarez, J. Matas, A. Álvarez-Bautista, J. Poejo, C. M. Duarte, L. Ruiz-Rubio, J. L. Vila-Vilela and L. M. León, *Carbohydr. Polym.*, 2016, **142**, 149–157.
- 31 N. Alizadeh and F. Nazari, *J. Mol. Liq.*, 2022, **346**, 118250.
- 32 A. Marchese, I. E. Orhan, M. Daglia, R. Barbieri, A. Di Lorenzo, S. F. Nabavi, O. Gortzi, M. Izadi and S. M. Nabavi, *Food Chem.*, 2016, **210**, 402–414.
- 33 W. Zhou, Y. Zhang, R. Li, S. Peng, R. Ruan, J. Li and W. Liu, *Foods*, 2021, **10**, 1074.
- 34 R. Najafloo, M. Behyari, R. Imani and S. Nour, *J. Drug Delivery Sci. Technol.*, 2020, **60**, 101904.



- 35 A. Garg, J. Ahmad and M. Z. Hassan, *J. Drug Delivery Sci. Technol.*, 2021, **64**, 102609.
- 36 S. Dou, Q. Ouyang, K. You, J. Qian and N. Tao, *Postharvest Biol. Technol.*, 2018, **138**, 31–36.
- 37 J. Stadermann, H. Komber, M. Erber, F. Däbritz, H. Ritter and B. Voit, *Macromolecules*, 2011, **44**, 3250–3259.
- 38 P. Jiao, H. Zhou, M. Otto, Q. Mu, L. Li, G. Su, Y. Zhang, E. R. Butch, S. E. Snyder, G. Jiang and B. Yan, *J. Am. Chem. Soc.*, 2011, **133**, 13918–13921.
- 39 L. Ouyang, L. Zhu, Y. Ruan and H. Tang, *J. Mater. Chem. C*, 2015, **3**, 7575–7582.
- 40 A. Celebioglu, F. Topuz, Z. I. Yildiz and T. Uyar, *Carbohydr. Polym.*, 2019, **207**, 471–479.
- 41 S. Botasini and E. Méndez, *J. Nanopart. Res.*, 2013, **15**, 1526.
- 42 S. Pande, S. K. Ghosh, S. Praharaj, S. Panigrahi, S. Basu, S. Jana, A. Pal, T. Tsukuda and T. Pal, *J. Phys. Chem. C*, 2007, **111**, 10806–10813.
- 43 T. Premkumar and K. E. Geckeler, *New J. Chem.*, 2014, **38**, 2847.
- 44 P. F. Andrade, A. F. de Faria, D. S. da Silva, J. A. Bonacin and M. D. C. Gonçalves, *Colloids Surf., B*, 2014, **118**, 289–297.
- 45 H.-J. Schneider, F. Hacket, V. Rüdiger and H. Ikeda, *Chem. Rev.*, 1998, **98**, 1755–1786.
- 46 M. A. Huq, M. Ashrafudoulla, M. M. Rahman, S. R. Balusamy and S. Akter, *Polymers*, 2022, **14**, 742.
- 47 N. Tarannum, D. Kumar and N. Kumar, *ChemistrySelect*, 2022, **7**, e202200140.

